Bearing Capacity of Transversely Prestressed Concrete Deck Slabs

Amir, Sana; van der Veen, Cor; Walraven, Joost C.; de Boer, Ane

Important note
To cite this publication, please use the final published version (if applicable).
Please check the document version above.
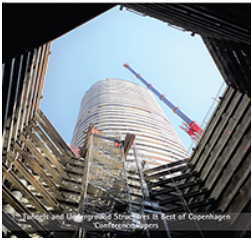
Bearing Capacity of Transversely Prestressed Concrete Deck Slabs

Sana Amir (Assistant Professor), Cor van der Veen , Joost C. Walraven & Ane de Boer

Published online: 03 Feb 2020.

Submit your article to this journal ☞

View related articles ☞

View Crossmark data ☞

Bearing Capacity of Transversely Prestressed Concrete Deck Slabs

Sana Amir (iD), Assistant Professor, Faculty of Engineering and Information Sciences, University of Wollongong in Dubai, Dubai, United Arab Emirates; **Cor van der Veen**; **Joost C. Walraven,** Department Design and Construction, Structural and Building Engineering, Concrete Structures, Faculty of Civil Engineering and Geosciences, Delft University of Technology, Delft, The Netherlands; **Ane de Boer,** Civil engineer and former employee of Ministry of Infrastructure and the Environment (Rijkswaterstaat), The Netherlands. Contact: sanaamir@uowdubai.ac.ae

Abstract

The Netherlands has a large number of thin, transversely prestressed concrete bridge decks, cast in-situ between flanges of prestressed concrete girders dating back to the 1960s and 1970s. These bridges are critical in shear when analyzed using EN 1992-1-1:2005; however, in reality, they show no significant signs of distress, possibly because of residual bearing (punching shear) capacity arising from compressive membrane action. Since these bridges are old, it is an astute approach to check whether they can be used for a few more decades, provided they are safe and reliable against modern traffic loads. The results could then be applied to a wider range of structures, especially in developing countries facing economic constraints. A prototype bridge was selected and experimental, numerical and theoretical approaches were used to investigate its bearing capacity. Respective coefficients of variation of 11% and 9% were obtained when the experimental and the finite element analysis punching loads were compared with the theoretical results. This led to the conclusion that the existing transversely prestressed concrete bridge decks still have sufficient bearing capacity and considerable cost savings can be made if compressive membrane action is considered in the analysis.

Keywords: bridge decks; transverse prestressing; punching shear; compressive membrane action; nonlinear analysis

Introduction

Are the old structures safe? Do old bridges have sufficient capacity to carry the present traffic loads? If the bridges designed according to old codes and requirements still seem to be in working condition, where is the residual capacity coming from?

These are questions that structural engineers and designers are facing all over the world, since the construction boom of the latter half of the twentieth century left the world with costly structures that have now become old and may or may not be adequate according to modern design requirements. Since complete demolition of these expensive structures, and then replacing them with new ones, would be a huge burden on the economy, it is an astute approach to check whether these structures can still be used for a few more decades provided they are safe and viable. A filter can be developed regarding structures that need to be replaced completely, structures that only need to be retrofitted for functioning, or structures that have sufficient residual capacity that makes them serviceable for another stretch of time.

The current research deals with the problem introduced above, with a focus on the bridges in the Netherlands; in particular, bridges with thin transversely prestressed decks cast in-situ between the flanges of long, precast girders. There are around 70 such bridges in the Netherlands that were constructed in the 1960s or 1970s. Since the traffic flow has increased enormously since then, the safety of old bridges has become questionable according to the modern design codes. In addition, the shear capacity as prescribed by the codes is more conservative in the recently implemented EN 1992-1-1:2005[1] than in the formerly used Dutch NEN 6720:1995.[2] As a result, many existing bridges are found to be shear-critical when assessed using the Eurocode. In 2006, the Dutch Ministry of Infrastructure and the Environment, Rijkswaterstaat, carried out a review of the old bridges of the Netherlands and found that most of the bridges were in good condition despite being loaded beyond their calculated capacity. Possible explanations for this anomaly could be the increase in the concrete strength as a result of ongoing cement hydration over the years, the transverse load redistribution in slabs and, most importantly, the well-recognized but yet to be validated "compressive membrane action" (CMA) or the dome effect. Basically, when a load is applied on a laterally restrained slab, its edges tend to move outwards and the boundary elements produce a compressive membrane force in the plane of the slab, enhancing the bearing capacity in both flexure and punching shear (*Fig. 1*).[3] As concluded by various researchers,[4–8] CMA is also the reason why bridges that are traditionally designed by conservative flexural theories mostly fail in
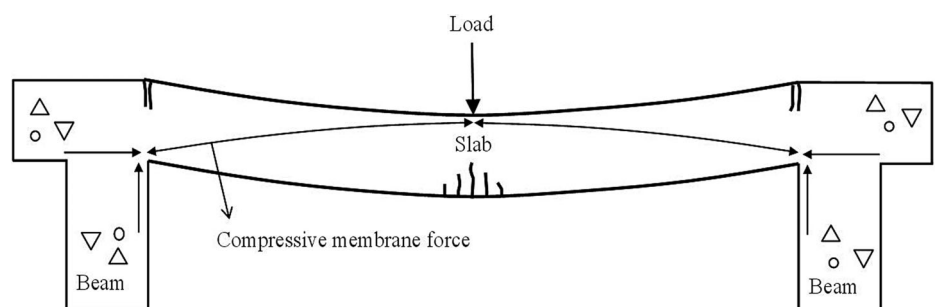
Fig. 1: Compressive membrane action in a reinforced concrete bridge deck slab [adapted from Ref. 3]

punching shear rather than in flexure under concentrated wheel loads. Therefore, when analyzing bridge deck slabs considering CMA, the punching shear capacity becomes the most critical aspect of the structural behavior.

Punching Shear

Punching shear failure is a combined action of flexure and shear load resulting in flexural, radial and inclined shear cracking. In slab–column specimens, the punching failure is categorized by a cone of concrete around the column plugging out of the surrounding slab. The behavior of bridge deck slabs under concentrated loads is not only different from that of slab–column specimens but more complex as well. In deck slabs, the punching shear mechanism may not be truly symmetrical since the flow of inner forces is different from that observed in slab–column specimens. The transverse spans are much smaller than the longitudinal spans and a perfect conical failure plug may not develop. Furthermore, in deck slab, depending on the aspect ratio of the loading block, failure can range from brittle punching to more ductile behavior, meaning that it has large deflections and rotations. However, the final failure mode is always punching.

Research Aim and Hypothesis

A lot of research has been carried out on the subject of CMA in reinforced concrete slabs and deck slabs. Codes such as those in Refs. [9–11] have incorporated membrane action in their analysis and design provisions to some extent. However, not much research has been conducted on prestressed concrete decks considering CMA, nor have any codes incorporated membrane action in their prestressed slab analysis and design methods. Furthermore, codes used in the Netherlands do not consider the beneficial effect of CMA in their design provisions at all. Therefore,

the scope of this research work covers the structural behavior and ultimate bearing capacity; in particular, the punching shear capacity of typical transversely prestressed decks under concentrated loads considering CMA. Since both transverse prestressing and CMA create compressive forces in the plane of a prestressed, laterally restrained slab, the hypothesis of this research can be stated as:

The in-plane compressive forces from transverse prestressing in combination with the compressive membrane forces arising from the lateral restraint will enhance the bearing capacity of bridge decks.

It is worth noting here that the slenderness ratio of such bridge decks is quite high, defying the slenderness limitation for the development of CMA in codes including Refs. [9–11]. However, since these codes are for reinforced concrete deck slabs, it is expected that the transverse prestressing will not only improve the bearing capacity but also compensate for the high slenderness ratio, making thinner deck slabs possible with no problems of serviceability and structural safety.

To prove the hypothesis, experimental, numerical and theoretical approaches were employed and a comparison was drawn at the end. Nineteen experiments were conducted in the Stevin II Laboratory, Faculty of Civil Engineering and Geosciences, Delft University of Technology, to investigate the capacity of a 1:2 scaled model of a bridge with a thin transversely prestressed concrete deck slab, cast between precast concrete girders and subjected to concentrated loads. A three-dimensional (3D) solid finite element model of the same bridge was developed in TNO DIANA FX+ 9.4.4[12] and several nonlinear analyses were carried out to study the punching behavior. A theoretical analysis concluded the research by making some modifications to the critical shear crack theory (CSCT)[13,14] as given in the Model Code 2010[15] for prestressed slabs. This paper briefly describes the

experiments and the finite element analysis (FEA) results while focusing primarily on the theoretical analysis and comparison.

Experimental Investigation

A comprehensive experimental program was conducted in the laboratory on a half-scale model of a real approach bridge (*Fig. 2*) in the Netherlands. This section briefly describes the design and construction of the model bridge deck and the experimental program.

Real Bridge

The prototype used in the research was based on the "approach" of the Van Brienenoord bridge, which was constructed in 1965 and connects the city of Rotterdam with the southern part of the Netherlands by crossing the River Nieuwe Maas (*Fig. 3*). In a typical Dutch "approach" bridge, the deck slab is quite slender and is cast in-situ between the flanges of precast, prestressed concrete girders. The interface between the deck slab and the girder is indented to generate sufficient interface shear capacity. The regular reinforcement ratio of the deck slab is quite low as prestressing reinforcement is already present. The prestressing tendons in the slab are placed in the transverse direction at an average spacing of around 650 mm center-to-center (c/c). At the location of the anchors, the spacing between the longitudinal tendons in the girders is 800 mm c/c. Transversely prestressed end transverse beams are present at the supports, along with diaphragms at one-third and two-thirds of the span. The bridge decks have been cast with concrete of normal strength; however, currently the concrete strength is considerably higher as a result of ongoing cement hydration over the years.[16] More details regarding the real bridge can be found in Ref. [17].
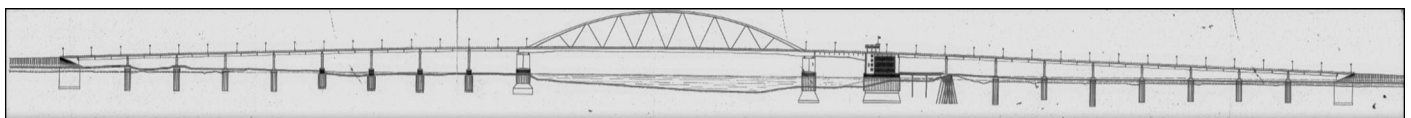
Fig. 2: Old draft drawing of the Van Brienenoord bridge in Rotterdam, consisting of nine approach spans of 50 m, an arch bridge of 300 m, the bascule bridge, the bascule pit and another nine approach spans of 50 m

Fig. 3: Aerial view of the Van Brienenoord bridge (taken from https://beeldbank.rws.nl/MediaObject/Details/312051)

Prototype of the Bridge

To simulate the actual bridge as closely as possible, a 1:2 scale was used to design the prototype. Linear scale factors,[17] based on the geometry and keeping the stress as unity in the real and the prototype bridge, were used to derive the scale factors of the prototype. The effect of size was considered when applying the results of the prototype to the full-scale bridge.[17] The girders and the deck slab were designed in such a way that failure would occur in the deck slab, as it was the slab which was the main interest in this research. The design calculations of the prestressing reinforcement required in the girders and the deck slab are provided in Ref. [18].

Test Set-up

Figures 4 and 5 show the test specimen representing the prototype bridge. The deck was 6.4 m wide and 12 m long, with a main span of 10.95 m and a cantilever of 525 mm at each end. It consisted of four, 1300 mm high, precast concrete girders placed at 1800 mm c/c distance. The three deck slab panels, with a clear transverse span of 1050 mm and a thickness of 100 mm, were cast in-situ between the flanges of the girders and post-tensioned in the transverse direction. Two transverse beams were provided at

Fig. 4: The 1:2 scale model bridge deck in the laboratory (Photo: authors)
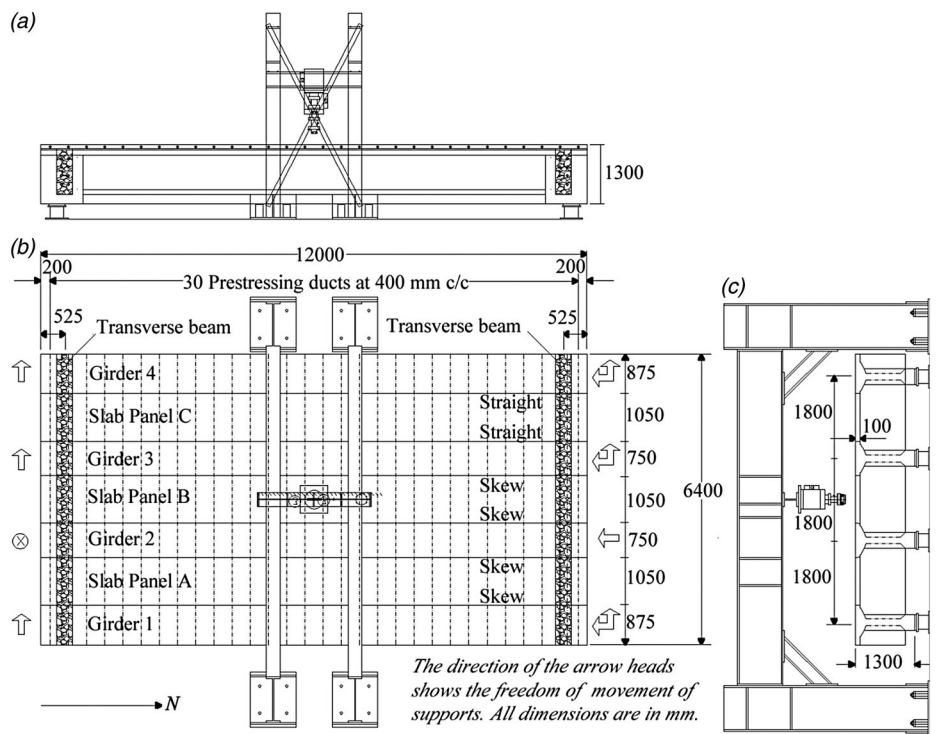
Fig. 5: Overview of the laboratory test set-up: (a) longitudinal view; (b) top view; (c) transverse view

525 mm from the end of the girder–deck slab assembly and were post-tensioned in the transverse direction at the same level as the deck slab. Some specific details of the girders are shown in Fig. 6. The exterior girders had an extended width of 125 mm at the exterior flanges to make sure that the prestressing and the confining effect were introduced adequately. Some of the interfaces between the deck slab panel and the girder flange were skew (1:20) and their location in plan is shown in Fig. 5b. A teardrop pattern of size 30 × 10 mm with 1–2 mm depth (Fig. 6d) was selected for the interface joint classified as "smooth" according to Eurocode 2. This pattern was introduced by placing specially formed shear keys in the molds.

In the deck slab, regular steel reinforcement was provided at both the top and bottom of the slab with 6 mm diameter bars at 200 mm c/c in the longitudinal direction and 6 mm diameter bars at 250 mm c/c in the transverse direction. A 7 mm concrete cover was provided on all sides in the deck slab. The transverse prestressing steel consisted of 15 mm diameter unbonded bars post-tensioned to the desired level. The prestressing bars were provided at the mid-depth of the deck slab at a uniform spacing of

400 mm c/c. The prestressing level was monitored to record any losses that could occur in time.

Design Lower Bounds

To consider the most unfavorable effects in the investigation, the following lower bounds were considered during design.

- In the real bridge, the interface between the side of the upper flange of the girder and the cast in-situ deck is inclined to 5 degrees at one side of the deck slab but the prototype was provided with inclined (skewed) interfaces at both sides of two out of three deck slab panels (Fig. 5b).
- The spacing of the transverse prestressing tendons was increased from the general spacing of 650 mm c/c in the actual bridge to 800 mm c/c (scaled down to 400 mm c/c in the prototype).
- Most of the tests were performed with a load applied in-between two adjacent transverse prestressing ducts in the deck. It has been shown in the literature[19] that testing directly above a duct gives a higher capacity than testing in-between the ducts.
- Three transverse prestressing levels (TPLs) were applied: 0.5, 1.25 and
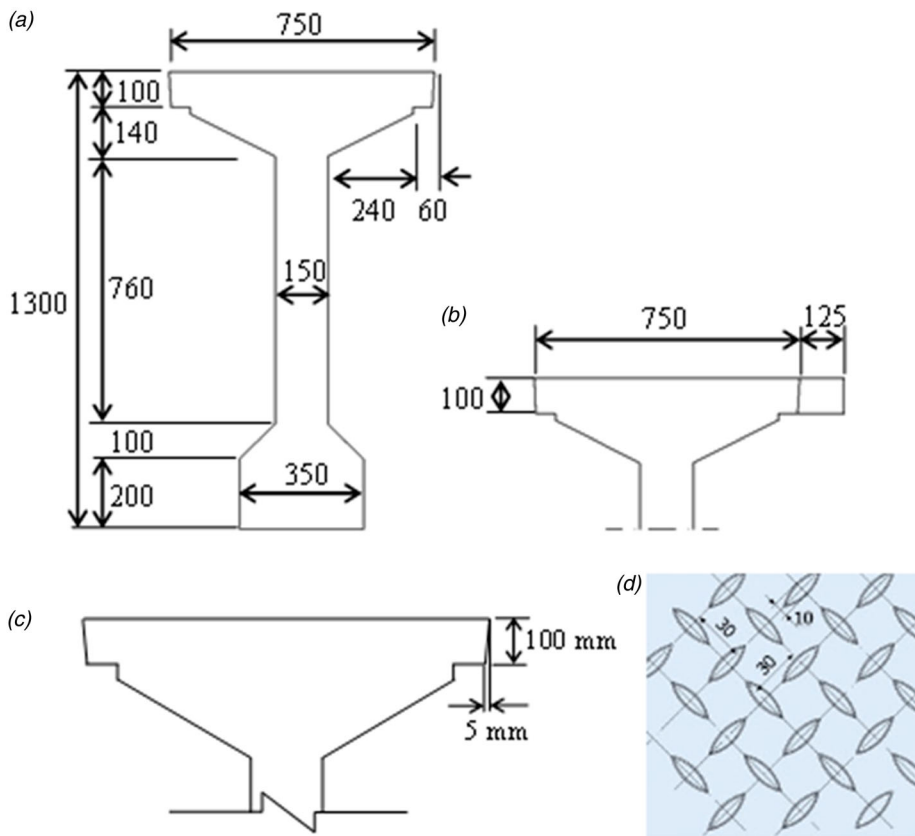
Fig. 6: Cross-section detail of the girders and interfaces shared with the deck slab: (a) model bridge interior girder; (b) model bridge exterior girder with extended flange width of 125 mm; (c) skewness of the girder flange interface; (d) roughness: Ruukki® DIN 59220 teardrop pattern used to produce the indented interface between the girder flange and deck slab

2.5 MPa. Although the usual TPL in a real bridge is 2.5 MPa, a TPL of 1.25 MPa was applied to simulate the eventual effect of tendon failure. The TPL of 0.5 MPa was applied to simulate a reinforced concrete bridge deck with a very limited effect of prestressing.

- To adjust the prestressing level, unbonded prestressed bars were applied in the deck slab, whereas in the real bridge only bonded cables are present.
- Although the prototype was provided with two transverse beams at each end, no diaphragms were present owing to the limited length of the bridge deck.

Load Application

A concentrated load simulating a wheel print load was applied by the hydraulic actuator attached to an overhead reaction frame bolted to the floor (*Fig. 5*). The load (*Fig. 7*) was according to Eurocode 1 Load Model 1, EN 1991-2:2002,[20] and the wheel print of 400×400 mm was scaled down according to 1:2. The

double load consisted of two wheel print loads placed at a distance of 600 mm c/c, scaled down from 1200 mm c/c. In the entire testing program, the load was applied through a 200×200 mm, 8 mm thick rubber bonded to two $200 \times 200 \times 20$ mm steel plates. For details of the instrumentation, reference is made to Refs. [17, 21].

Material Properties

The concrete compressive strength was measured on cubes and converted to cylinder strength as per EN 1992-1-1:2005 (EC 2)[1] and the tensile strength was measured by the splitting tensile strength test. For the deck slab and the transverse beams, the mean compressive cylinder strength f_{cm} of concrete was 65 MPa, the mean splitting tensile strength f_{csp} was 5.41 MPa and the mean modulus of elasticity E_{cm} was calculated as 39 GPa (EC2). For the girders, the mean compressive cylinder strength f_{cm} of concrete was 75 MPa, the mean splitting tensile strength f_{csp} was 6.30 MPa and the mean modulus of elasticity E_{cm} as per EC2 was

41 GPa. The steel reinforcement had a yield strength f_{sy} of 525 MPa and modulus of elasticity E_s of 200 GPa, and the prestressing steel had a characteristic tensile strength f_{pk} of 1100 MPa. The material properties are collected in *Table 1*. Since the experimental program started approximately 3 months after casting the deck slab and approximately 9 months after casting the girders, an average of the mean strengths after 28 days until the last test was used.

Test Parameters

The test configuration and parameters are collected in *Table 2*. *Figure 8* shows the location of the loads in various tests; the numbers are marked according to the sequence of the tests performed. Generally speaking, four types of tests were performed:

- P1M: single wheel print load acting at the midspan of the deck slab panel
- P1J: single wheel print load acting close to the girder flange–deck slab interface/joint
- P2M: double wheel print loads at 600 mm c/c acting at the midspan of the deck slab panel
- P2J: double wheel print loads at 600 mm c/c acting close to the girder flange–deck slab interface/joint.

Both exterior (A and C) and interior (B) deck slab panels (see *Fig. 6*) were tested at several locations along the length of the deck. For most of the interface (J) tests, the load was applied at 200 mm from the interface (c/c), with the exception of tests BB3 and BB4, where the center of the loading plate was at 110 mm from the interface. Sixteen out of 19 tests were performed by placing the center of the loading plate in-between the transverse prestressing ducts (BD). The remaining three tests were carried out with the load just above a duct (AD). The size of the loading plate was 200×200 mm in all the tests, with the exception of test BB19, where a small loading plate (SLP), 115×150 mm, was used.

Numerical Investigation

Most of the research work carried out in the past to study CMA in reinforced and prestressed concrete slabs focused on small-scale experiments. Two major
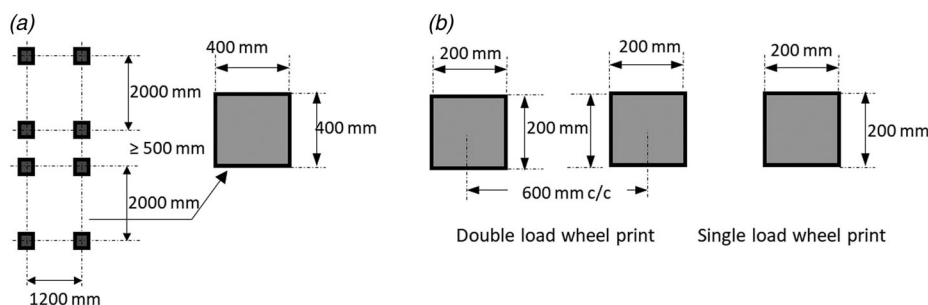
Fig. 7: (a) Eurocode load configuration and wheel print (load model 1, EN 1991-2:2002); (b) single and double load wheel print according to the Eurocode scaled down to 1:2

Component	Material	Property	Value
Deck slab and transverse beams	Concrete	Mean compressive cylinder strength, f_{cm} [MPa]	65
		Mean tensile strength, f_{ctm} [MPa]	5.41
		Modulus of elasticity, E_{cm} – EC2 [GPa]	39
	Prestressing steel	Characteristic tensile strength, f_{pk} [MPa]	1100
		Characteristic 0.1% proof stress, $f_{p0.1k}$ [MPa]	900
		Modulus of elasticity, E_p [GPa]	205
	Ordinary steel	Mean yield strength, f_{sy} [MPa]	525
		Mean ultimate tensile strength, f_{su} [MPa]	580
		Modulus of elasticity, E_s [GPa]	200
Girders	Concrete	Mean compressive cylinder strength f_{cm} [MPa]	75
		Mean tensile strength, f_{ctm} [MPa]	6.3
		Modulus of elasticity, E_{cm} – EC2 [GPa]	40.26

Table 1: Material properties of various components of the model bridge

reasons for not conducting large-scale testing are the costs associated with it and the lack of space in the laboratory. The main drawback of conducting small-scale experiments is the size effect that comes into play once the results are applied to actual cases. Therefore, it is essential that calibrated numerical models are developed that are able to predict the actual structural behavior. Furthermore, numerical models can be used to carry out a parametric study which may not be possible experimentally owing to the high costs associated with the construction and testing of physical models. The main objective of carrying out the numerical analysis was to determine the bearing (punching shear) capacity as well as the in-plane forces arising from the combined effect of transverse prestressing and CMA. The details of the numerical modeling can be found in Refs. [17, 22].

The 3D Solid Finite Element Model

For the numerical analysis, a 3D solid finite element model of the prototype bridge deck (*Figs. 9, 10*) was constructed in the FEA software package DIANA (FX+ 9.4.4).[12] The model consisted of 3D solid quadratic elements (CHX60 and CTP45) with a fine mesh around the loading area and a coarse mesh away from the loading to reduce the time for computation. A layer of composed quadratic elements (CQ8CM) was provided in the fine mesh area to calculate the in-plane forces arising from the combined effect of transverse prestressing and

CMA. (The in-plane forces were later used in the theoretical model to study the effect of transverse prestressing and compressive membrane forces on the bearing capacity.) Ducts at 400 mm c/c were provided only in the fine mesh area around the loading. Prestressing pressure was applied according to the required TPL in the deck slab and the transverse beams. For most cases the deck slab was analyzed nonlinearly, while the girders and the transverse beams remained in the linear range since it was known from the experiments that the girders and the transverse beams do not show any nonlinear behavior. The only exceptions to this were tests BB3 and BB4. The flange of the adjoining girder was analyzed as nonlinear since the experimental load was too close to the interface (110 mm c/c) and linearity of the flange in the numerical model would have induced a much higher capacity than in reality. An embedded reinforcement grid, based on the actual reinforcement, was provided in the deck slab panels at the top and bottom in the horizontal as well as the vertical direction.

Material Models and Additional Nonlinear Material Properties

For the basic material properties of the deck slab, girders and transverse beams, reference is made to the experimental investigation described earlier in the article. For the nonlinear analysis of the deck slab, a smeared cracking "Total strain crack rotating model" was selected. An elastic–perfectly plastic model, CONSTA, was used for the concrete behavior in compression, whereas an exponential softening curve, HORDIJK, was used for the concrete behavior in tension. A fracture energy G_f of 0.15 N/mm was assumed for the deck slab concrete. The Poisson ratio v, for all of the concrete components, was taken as 0.2. For the embedded grid reinforcement, the von Mises plasticity criterion was used with a Poisson ratio of 0.3.

Iteration Method and Convergence Criteria

Both physical and geometric nonlinearities were applied to the system. An incremental–iterative procedure was used for the nonlinear analysis and a modified Newton Raphson method was used for the solution. The prestressing load was applied to the bridge

No.	Test	Panel	Load type	TPL [MPa]	Joint	Designation
1	BB1	C–Midspan	Single (BD)	2.5	Straight	C-P1M-ST
2	BB2	A–Midspan	Single (BD)	2.5	Skewed	A-P1M-SK
3	BB3	A–Interface	Single (BD)	2.5	Skewed	A-P1J-SK
4	BB4	C–Interface	Single (BD)	2.5	Straight	C-P1J-ST
5	BB5	C–Midspan	Double (BD)	2.5	Straight	C-P2M-ST
6	BB6	A–Interface	Double (BD)	2.5	Skewed	A-P2J-SK
7	BB7	C–Midspan	Single (BD)	2.5	Straight	C-P1M-ST
8	BB8	C–Midspan	Single (BD)	1.25	Straight	C-P1M-ST
9	BB9	A–Midspan	Single (BD)	1.25	Skewed	A-P1M-SK
10	BB10	A–Interface	Single (BD)	1.25	Skewed	A-P1J-SK
11	BB11	C–Midspan	Double (BD)	1.25	Straight	C-P2M-ST
12	BB12	A–Interface	Double (BD)	1.25	Skewed	A-P2J-SK
13	BB13	C–Midspan	Single (AD)	1.25	Straight	C-P1M-ST
14	BB14	C–Interface	Single (AD)	1.25	Straight	A-P1J-ST
15	BB15	A–Midspan	Single (AD)	1.25	Skewed	A-P1M-SK
16	BB16	B–Midspan	Double (BD)	2.5	Skewed	B-P2M-SK
17	BB19*	B–Midspan	Single (BD)	2.5	Skewed	B-P1M-SK
18	BB21	B–Midspan	Single (BD)	0.5	Skewed	B-P1M-SK
19	BB22	B–Midspan	Single (BD)	0.5	Skewed	B-P1M-SK

*Small loading plate (115 × 150 mm); all other tests used a 200 × 200 mm loading plate.
TPL: transverse prestressing level; AD: above duct; BD: in-between two ducts; ST: straight joint; SK: skewed joint; P1M: single wheel print load acting at midspan of deck slab panel; P1J: single wheel print load acting close to the girder flange–slab interface/joint; P2M: double wheel print load acting at midspan of deck slab panel; P2J: double wheel print load acting close to the girder flange–slab interface/joint.

Table 2: Testing configuration
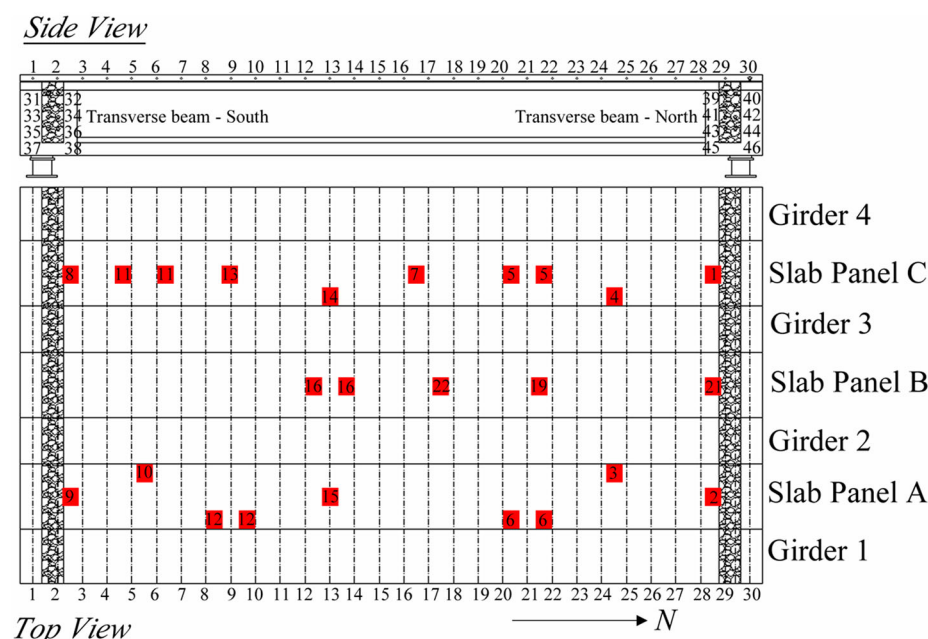
Fig. 8: Deck slab test positions (BB1–BB22). Duct positions are labeled with dotted lines

deck in a single step. After that, a displacement-controlled load was applied with a step size of 0.1 mm unless the solution diverged, in which case the displacement increment was reduced to 0.05 mm. Since the applied load was displacement controlled, the default force and energy-based convergence criterion was employed.

Theoretical Analysis

MC2010 Punching Shear Provisions Based on the CSCT

The Model Code 2010[15] punching shear provisions are based on the CSCT for reinforced concrete and pre-stressed concrete[13,14] slabs using the level of approximation (LoA) approach.[23] In this research, the same model was employed but with some modifications to include CMA. *Figures 11 and 12* show the basic mechanism of the CSCT without shear reinforcement. For the assessment of the punching shear capacity, an iterative procedure needs to be carried out to find the intersection point of the failure criterion described below and the load–rotation curve of the slab representing the available punching shear strength and the shear force for a given rotation, respectively.

Failure Criterion

Equation (1) gives the simplified failure criterion of the CSCT.[13,14] This equation does not involve any material factors and is based on mean strengths:

$$\frac{V_R}{b_o d_v \sqrt{f_{cm}}} = \frac{3/4}{1 + 15 \dfrac{\psi d}{d_{go} + d_g}} \quad (1)$$

where V_R is the shear strength, b_0 is the length of the control perimeter at $d_v/2$ of the edge of the supported area, d_v is the shear-resisting effective depth of the member, f_{cm} is the mean compressive strength of the concrete, ψ is the rotation, d is the flexural effective depth of the member, d_{g0} is the maximum aggregate size, and d_g is the reference aggregate size, equal to 16 mm.

The following general equation found in Refs. [13, 14] was used to calculate the rotation ψ in Eq. (1):

$$\psi = 1.5 \frac{r_s}{d} \frac{f_{sy}}{E_s} \left(\frac{m_s - m_P}{m_R - m_P}\right)^{1.5} \quad (2)$$
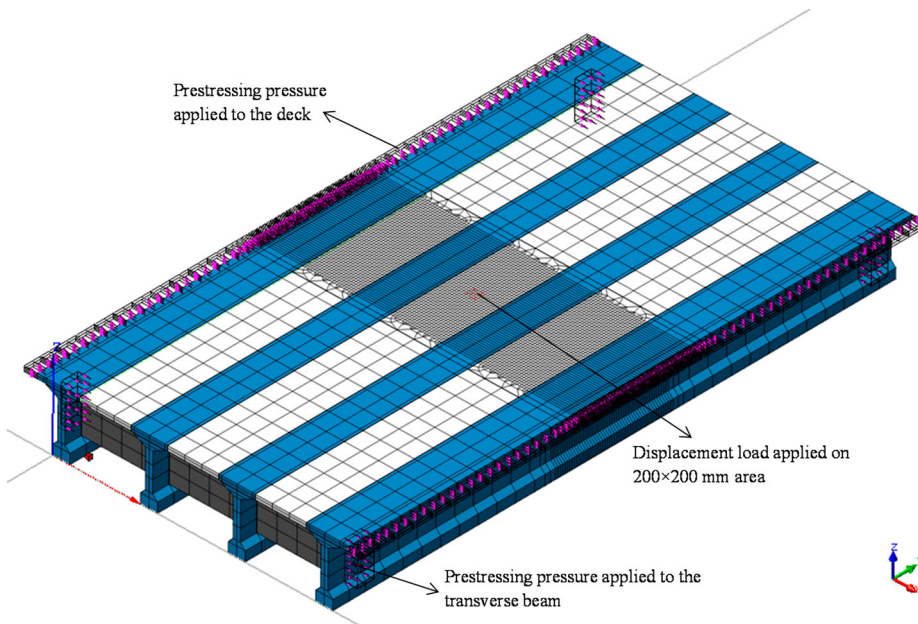
Fig. 9: Three-dimensional solid finite element bridge model for a typical P1M case
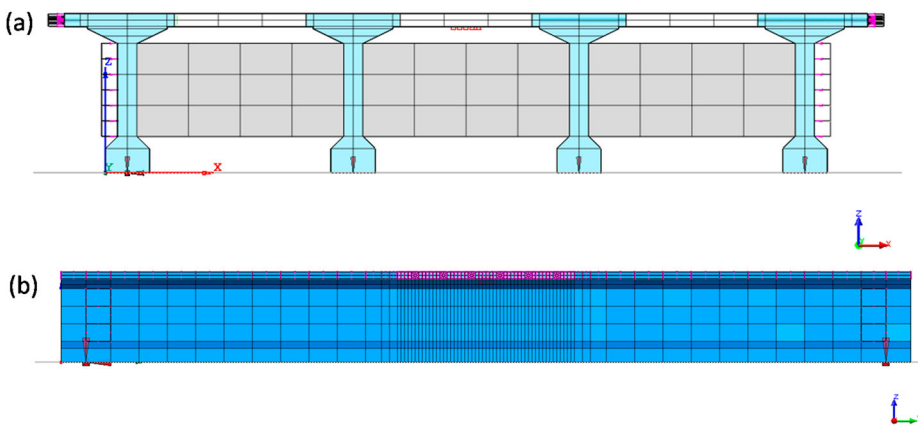
Fig. 10: Finite element bridge model for the basic test case analysis: (a) transverse cross-section; (b) longitudinal view
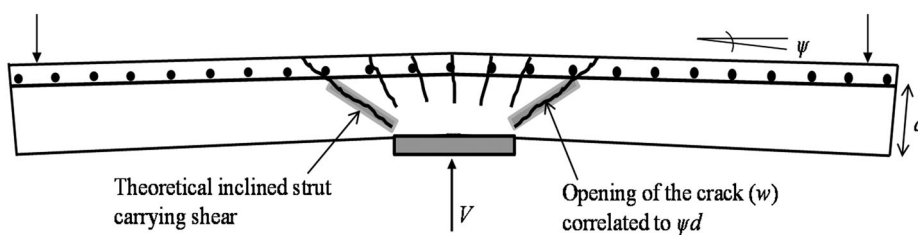
Fig. 11: Critical shear crack theory basic mechanism:[13] the width of the shear crack is assumed proportional to the product of the slab rotation times the effective depth of the slab ($w \propto d$)

where r_s refers to the distance from the axis of the column to the line of contraflexure of the bending moments; m_s is the average moment per unit length for the calculation of the flexural reinforcement in the support strip and $m_s \approx V/8$ for inner columns without unbalanced moments; m_R is the average flexural strength per unit length in the support strip and $m_R = \rho\ f_{sy}\ d^2\ (1 - 0.5\rho f_{sy}/f_{cm})$; m_P is the average decompression moment over the width of the support strip due to prestressing and $m_P = n\ (h/2 - d/3 + e)$. In these expressions, V is the acting shear force, ρ is the steel reinforcement ratio, f_{sy} is the yield strength of the steel, f_{cm} is the mean compressive cylinder strength of concrete, n is

the normal force per unit length, h is the depth of the slab, d is the effective depth, and e is the eccentricity of the normal force from the center of gravity of the section. As a sign convention, the decompression moment is considered positive when it leads to compressive stresses on the top side of the slab.

Proposed LoA Approach Using the CSCT

Since the original CSCT punching shear model does not include CMA, it was modified by combining it with the numerically found in-plane forces from the finite element model. It was expected that the in-plane forces arising from the combined effect of transverse prestressing and CMA will enhance the bearing capacity to an even larger extent. To study this phenomenon, two levels of approximation were introduced: (a) elementary LoA, and (b) advanced LoA.

Elementary LoA

The load–rotation relationship was established using the transverse prestressing force as the normal force n. This served as a lower bound for the ultimate capacity (*Fig. 13*).

Advanced LoA

The load–rotation relationship was established using the overall in-plane force (sum of transverse prestressing force and compressive membrane force) as the normal force n, found from the nonlinear analyses of the 3D solid, finite element model bridge (output N_{xx} from the composed elements).[17] This served as the upper bound of the ultimate capacity and CMA was automatically incorporated in the load–rotation relationship (*Fig. 13*).

Verification of the Proposed LoA Approach Using CSCT with Test Results from Past Literature

For the verification of the proposed model, the elementary and advanced LoA approach for the CSCT was applied on restrained, prestressed deck slabs or slabs from the literature. Where lateral restraint is low, the calculation is applied on the elementary level only.

Figure 14 shows the theory applied on eight experimental studies, comprising
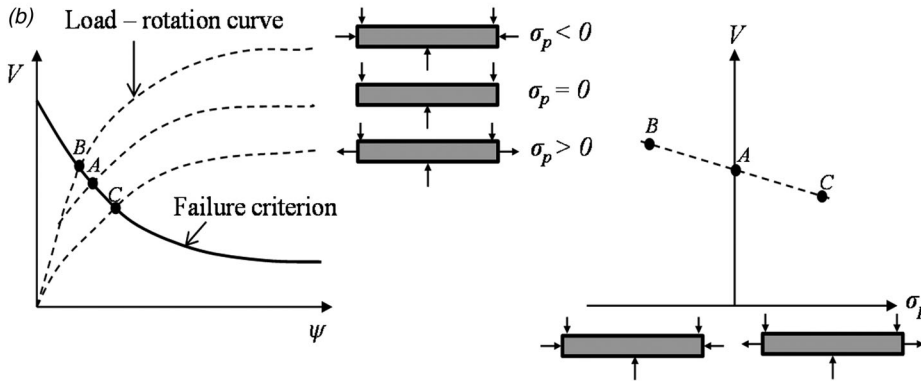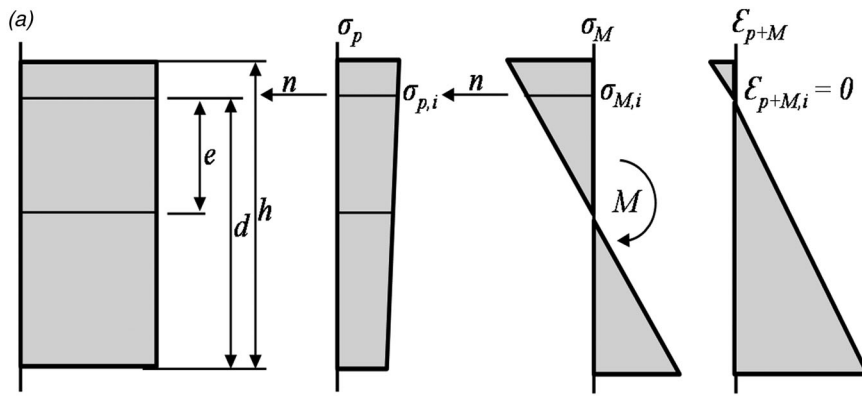
Fig. 12: Critical shear crack theory for prestressed slabs:[14] (a) section subject to in-plane normal force, state of associated stress, state of stress due to decompression moment, and resulting state of strain (from left to right); (b) influence of an in-plane force (σp) on the punching shear capacity, V

Fig. 13: Level of approximation (LoA) approach for analysis of the transversely prestressed deck slab). The elementary LoA gives punching shear load B and the advanced LoA gives punching shear load A. For no prestressing, the failure load is C. PS: prestressing; CMA: compressive membrane action

Fig. 14: Application of the proposed level of approximation (LoA) approach using critical shear crack theory (CSCT) on test results from past literature (details of these eight studies are given in Ref. [17]). CMA: compressive membrane action

56 tests that are similar in nature to the current experiments. All of the test cases cover transversely prestressed slabs (unbonded, bonded or external) and showed evidence of CMA arising from either the lateral restraints provided by the supports or external prestressing. The details of the investigated cases are given in Ref. [17]. The in-plane forces used in the calculations were obtained either experimentally or by FEA in these studies, or they have been assumed proportionally based on the in-plane forces obtained in the FEA of the current model under study. For instance, for tests conducted in Refs. [19, 24, 25] on a 1/4.04 scaled model with a 43 mm thick deck slab, 50% of the normal forces obtained by the FEA of the 1:2 scaled model bridge deck of the current study have been assumed to be developed. The assumption is valid since sufficient CMA was witnessed in these tests and the bearing capacity was found to be much higher than expected. It can be observed that a coefficient of variation of 10% was obtained when the punching loads calculated by the

CSCT were compared with the experimental results.

Application of the Proposed Model to the Research Problem

When applying the CSCT to the model bridge deck, mean values of material strengths were used with no material factors in Eq. (1). For openings and inserts, the basic control perimeter b_0 is recommended to be reduced[14] but the presence of ducts in the current problem has been ignored while calculating b_0. *Figure 15* shows the critical shear perimeters being considered. For single loads, Model Code 2010[15] considers the critical shear perimeter at half the effective depth from the face of the loaded area. For the double load cases, the perimeters of the two loaded areas are combined. The flexural effective depth of the section was taken to be equal to the shear resisting effective depth in the assessment calculations ($d = d_v = 87$ mm). For calculation of m_P in Eq. (2), no eccentricity exists since the prestressing bars are applied at mid-depth. Furthermore, ρ_{ps} (geometric prestressing steel ratio) and
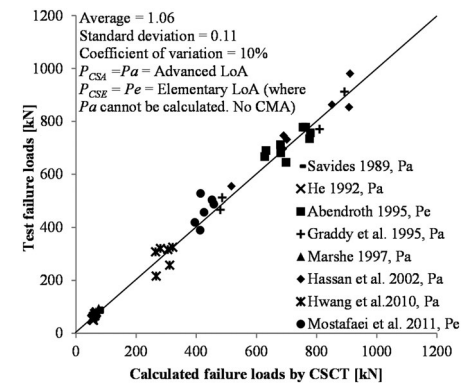
f_{pe} (effective prestress) representing an equivalent steel were used in place of ρ and f_{sy}, respectively, to determine the flexural strength m_R of the deck slab panel with unbonded transversely prestressed bars in Eq. (2). Equation (3)[17] was used to determine the equivalent steel ratio:

$$\rho_{eq} = \frac{\rho_{ps} \, f_{pe}}{f_y} \qquad (3)$$

where ρ_{eq} is the equivalent reinforcement ratio, ρ_{ps} is the geometric ratio of the prestressed reinforcement, f_{pe} is the effective prestress of the tendons, and f_y is the yield strength of the non-prestressed reinforcement. A MATLAB® program[17] was developed to make the iterative calculations and
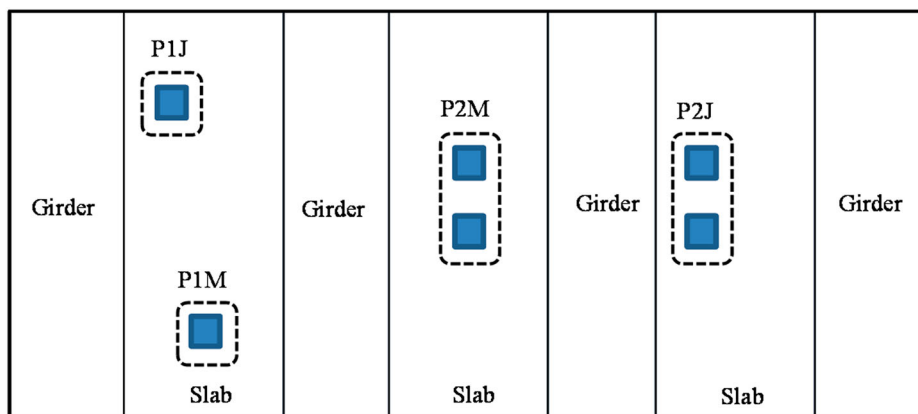
Fig. 15: Determination of critical shear perimeter for various load cases at a distance d/2 from the face of the loaded area (Model Code 2010[15])

Fig. 16: Graphical representation of the critical shear crack theory level of approximation (LoA) approach for P1M load case at the elementary LoA with only prestressing forces (MATLAB output)

Fig. 17: Graphical representation of the critical shear crack theory level of approximation (LoA) approach for P1M load case at the advanced LoA with prestressing and compressive membrane action (CMA) (MATLAB output)

Test BB	TPL [MPa]	Designation Panel–load type	Normal force, n [N/mm]	Miscellaneous
1	2.5	C–P1M	615	$f_{cm} = 65$ MPa
2	2.5	A–P1M	615	$E_s = 200$ GPa
3	2.5	A–P1J	1668*	$d_g = 20$ mm
4	2.5	C–P1J	1668*	$B = 1050$ mm
5	2.5	C–P2M	678	$b_c = 200$ mm
6	2.5	A–P2J	681	$c_c = 200$ mm for single loads
7	2.5	C–P1M	615	and 800 mm for double loads
8	1.25	C–P1M	501	$d = 87$ mm
9	1.25	A–P1M	501	
10	1.25	A–P1J	614	From FEA:
11	1.25	C–P2M	555	$r_s = 250$ mm ($\approx$ B/4, assuming maximum rotations occur in the transverse direction)
12	1.25	A–P2J	556	
16	2.5	B–P2M	867	
19	2.5	B–P1M (SLP)	708	n = depends on TPL and CMA, found from FEA (N_{xx} of composed elements)

*The center of the loaded area was too close to the girder flange–deck slab interface in the finite element analysis (FEA) (150 mm); hence these cases show very high in-plane forces.
TPL: transverse prestressing level; SLP: small loading plate; CM: compressive membrane action.

Table 3: Input for the MATLAB program to estimate the ultimate capacity using critical shear crack theory

plot the load–rotation curves against the failure criterion for the model bridge deck. The possibility of flexural failure was ruled out of the iterative procedure, since no such failure was observed in the tests or the FEA. Tests conducted above the ducts and the control tests with 0.5 MPa TPL were not considered. It should also be noted that the mean concrete strength of the girders ($f_{cm} = 75$ MPa) is higher than that of the deck slab panels ($f_{cm} = 65$ MPa), which means that a higher bearing capacity exists when the deck slab is loaded close to the interface, but this effect was ignored in the calculation. The input for the MATLAB program to assess the ultimate bearing (punching shear) capacity is collected in Table 3. Figure 16 shows typical the load–rotation behavior for a single load at the midspan (P1M) with a TPL of 2.5 MPa at an elementary LoA and Fig. 17 shows the same load case but for an advanced LoA. The failure criterion remains the same for both cases but the load–rotation behavior changes owing to a different contribution of the in-plane forces arising either from only prestressing, or from prestressing and CMA. Smaller rotation and consequently a higher punching load is obtained when considering CMA in the load–rotation behavior.
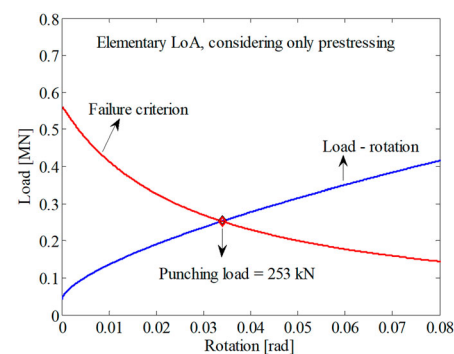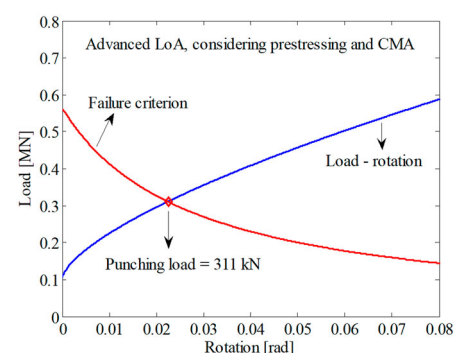
Comparison of Theoretical, Experimental and FEA Punching Loads

A comparison was drawn between the punching shear capacity obtained theoretically from the CSCT model and the results of the experimental and FEA (Table 4). Coefficients of variation of 11% and 9%, respectively, were obtained when the experimental and the FEA punching loads were compared with the advanced LoA results. The theoretical analyses based on the CSCT show that the mechanical model satisfies the experimental and numerical results fairly well and shows a better correlation with the advanced LoA that includes CMA.

Test BB	TPL [MPa]	Designation	P_T [kN]	P_{FEA} [kN]	P_{CSE} [kN]	P_{CSA} [kN]	P_T/ P_{FEA}	P_T/ P_{CSA}	P_{FEA}/ P_{CSA}
1	2.5	C–P1M	348.7	302.3	253	311	1.15	1.12	0.97
2	2.5	A–P1M	321.4	302.3	253	311	1.06	1.03	0.97
3	2.5	A–P1J	441.6	429.9	253	422.4	1.03	1.05	1.02
4	2.5	C–P1J	472.3	429.9	253	422.4	1.10	1.12	1.02
5	2.5	C–P2M	490.4	529.9	362.2	453.3	0.93	1.08	1.17
6	2.5	A–P2J	576.8	537.0	362.2	482.3	1.07	1.20	1.11
7	2.5	C–P1M	345.9	302.3	253	311	1.14	1.11	0.97
8	1.25	C–P1M	284.5	271.4	220.2	295.7	1.05	0.96	0.92
9	1.25	A–P1M	258.2	271.4	220.2	295.7	0.95	0.87	0.92
10	1.25	A–P1J	340.3	300.7	220.2	310.9	1.13	1.09	0.97
11	1.25	C–P2M	377.9	453.4	314.7	431.3	0.83	0.88	1.05
12	1.25	A–P2J	373.7	454.9	314.7	432.1	0.82	0.86	1.05
16	2.5	B–P2M	553.4	592.7	362.2	482.3	0.93	1.15	1.23
19	2.5	B–P1M	317.8	306.0	220.9	281.9	1.04	1.13	1.09
				Mean			1.02	1.05	1.03
				Standard deviation			0.11	0.11	0.09
				Coefficient of variation			0.11	0.11	0.09

TPL: transverse prestressing level; P_T: test punching failure load; P_{FEA}: finite element ultimate load; P_{CSE}: CSCT elementary level of approximation ultimate punching load; P_{CSA}: CSCT advanced level of approximation ultimate punching load.

Table 4: Comparison of the critical shear crack theory (CSCT) punching loads with the experimental and finite element analysis results

This proves that sufficient lateral restraint was available in the deck slab and the in-plane forces arising from a combined effect of transverse prestressing and CMA enhanced the bearing capacity. If a lower bound capacity is desired without carrying out a numerical analysis, the elementary LoA can be used. It can also be observed (*Table 4*) that increasing the TPL had a positive effect on the ultimate bearing (punching shear capacity). It is to be noted that both the experimental and numerical analyses showed that failure always occurred in punching shear and in the span of the slab, regardless of the number and position of the loads, and the interface between the girders and the deck slab remained safe.[17] The same assumptions were made while calculating the capacity theoretically and were verified through the model.

Conclusions

The detailed research results have led to the conclusion that the conventional bridge deck design and analysis methods are quite conservative and existing bridge decks have sufficient residual strength available to satisfy modern traffic demands. The in-plane compressive forces from transverse prestressing in combination with the compressive membrane forces arising from the lateral restraint give much higher bearing capacity than expected. The combined effect of prestressing and CMA can significantly enhance the bearing capacity and is the reason behind the residual capacity of existing structures. Furthermore, while experimental testing on large-scale models is quite expensive, the numerical and theoretical approaches have proven to be quite cost effective and their accuracy has been verified by comparison with the experimental results.

With regard to the numerical analysis, it was shown that the punching shear failures can be reasonably modeled with nonlinear FEA of 3D solid models and using composed elements can lead to the determination of compressive membrane forces developed in a laterally restrained slab, which were previously difficult to determine using analytical techniques. Moreover, CMA was also successfully incorporated in the CSCT punching shear model using a new LoA approach. With a standard deviation of 11% or less, the results are quite reliable and the model can be applied confidently to other types of bridge decks and laterally restrained slabs. This approach is especially useful in countries with economic constraints and where old bridges have to be assessed for residual capacity. Sufficient saving in cost can be made if it is proven that these bridges are still safe and can be used for a few more decades.

Disclosure statement

No potential conflict of interest was reported by the authors.

ORCID

Sana Amir http://orcid.org/0000-0003-0550-573X

References

[1] EN 1992-1-1:2005. Eurocode 2—*Design of Concrete Structures—Part 1-1: General Rules and Rules for Buildings*. Comité Européen de Normalisation (CEN), Brussels, Belgium, 2005; 229.

[2] NEN 6720:1995. *Regulations for Concrete: Structural Requirements and Calculation Methods*. Dutch Normalisation Institute (NEN), 1995 (in Dutch). Netherlands.

[3] Hon A, Taplin G, Al-Mahaidi RS. Strength of reinforced concrete bridge decks under compressive membrane action. *ACI Struct. J.* 2005; **102** (3): 393–401.

[4] Kirkpatrick J, Rankin GIB, Long AE. Strength evaluation of M-beam bridge deck slabs. *Struct. Eng.* 1984; **62b**(3): 60–68.

[5] Batchelor BDV. Membrane Enhancement in Top Slabs of Concrete Bridges. Concrete Bridge Engineering, Performance and Advances. Routledge: London, 1990; 189–213.

[6] Bakht B, Jaeger LG. Ultimate load test of slab-on-girder bridge. *J. Struct. Eng.* 1992; **118** (6): 1608–1624.

[7] Fang IK, Lee JH, Chen CR. Behavior of partially restrained slabs under concentrated load. *ACI Struct. J.* 1994; **91**(2): 133–139.

[8] Mufti AA, Jaeger LG, Bakht B, Wegner LD. Experimental investigation of fibre-reinforced concrete deck slabs without internal steel reinforcement. *Can. J. Civ. Eng.* 1993; **20**(3): 398–406.

[9] Ontario Highway Bridge Design Code (OHBDC), 2nd edn, Ontario Ministry of Transportation (OMTC), Highway Engineering Division, Ontario, Canada, 1983.

[10] Transit New Zealand Ararau Aotearoa, New Zealand Bridge Manual, 2nd edn, 2003.

[11] UK Highways Agency BD 81/02, *Use of Compressive Membrane Action in Bridge Decks*, *Design Manual for Roads and Bridges*, 3(4), part 20, 2002; 20.

[12] DIANA. FX+. User's Manual 9.4.4. TNO Building and Construction Research, Delft, 2012.

[13] Muttoni A. Punching shear strength of reinforced concrete slabs without transverse reinforcement. *ACI Struct. J.* 2008; **105**(4): 440–450.

[14] Clément T, Ramos AP, Fernández Ruiz M, Muttoni A. Design for punching of prestressed concrete slabs. *Struct. Concr.* 2013; **14**: 157–167.

[15] Model Code 2010. Final Draft Volume I and II. fib 2012. Bulletin 65 and 66. 2012.

[16] Witteveen+Bos. *Materiaalonderzoek betonnen kunstwerken 37h-006-01 van brienenoord oost (tussenstorten)*, Technical report (in Dutch), the Netherlands, 2009.

[17] Amir S. *Compressive membrane action in prestressed concrete deck slabs*. PhD thesis. Delft University of Technology, Delft, the Netherlands, 2014.

[18] Vugts MWJ. *Experimental determination of bearing capacity of transversely prestressed concrete deck slabs*. Master's thesis. Delft University of Technology, the Netherlands, 2012.

[19] He W. *Punching behaviour of composite bridge decks with transverse prestressing*. PhD thesis. Queen's University, Kingston, Ontario, Canada, 1992.

[20] EN 1991-2:2002. Eurocode 1—*Actions on Structures—Part 2: Traffic loads on bridges*, *Comité Européen de Normalisation (CEN)*, Brussels, Belgium, 2002.

[21] Amir S, van der Veen C, de Boer A, Walraven JC. Experiments on punching shear behavior of prestressed concrete bridge decks. *ACI Struct. J.* 2016; **113**: 627–636.

[22] Amir S, van der Veen C, Walraven JC, de Boer A. Numerical investigation of the punching shear capacity of transversely prestressed concrete deck slabs. *Struct. Concr.* 2019; **20**(3), 1109–1122.

[23] Muttoni A, Fernández Ruiz M. The levels-of-approximation approach in MC 2010: application to punching shear provisions. *Struct. Concr.* 2012; **13**: 32–41.

[24] Marshe S, Green MF. Punching behavior of composite bridge decks transversely prestressed with carbon fibre reinforced polymer tendons. *Can. J. Civ. Eng.* 1999; **26**: 618–630.

[25] Savides P. *Punching strength of transversely prestressed deck slabs of composite I-beam bridges*. Master's thesis. Queen's University, Kingston, Ontario, Canada, 1989.